A Battery-free Pavement Roughness Estimation System Based on Kinetic Energy Harvesting

Hailiang Yang, Li Teng, and Junrui Liang
School of Information Science and Technology
ShanghaiTech University, Shanghai 201210, China
Email: {yanghl, tengli, liangjr}@shanghaitech.edu.cn

2022 IEEE International Symposium on Circuits and Systems (ISCAS) | 978-1-6654-8485-5/22/$31.00 ©2022 IEEE | DOI: 10.1109/ISCAS48785.2022.9937719

***Abstract*—Wireless sensor network (WSN) enables the continuous monitoring of environmental conditions. These systems are usually powered by batteries. Given that there might be tremendous distributed sensor nodes in a network, battery maintenance must become one of the major challenges for their massive deployment. Energy harvesting technology, by which energy is extracted from the ambient environment, is developed for powering the ubiquitous Internet of Things (IoT) devices using different types of local energy, such as solar, vibration, and wind. In this paper, based on the vibration energy harvesting technology, we introduce a battery-free pavement roughness estimation system (BF-PRES), which provides road roughness information by linking the driving vibration and wireless packet count. Instead of harvesting energy to power an off-the-shelf commercial accelerometer and implementing some algorithms for vibration estimation, BF-PRES simply sends out a BLE Beacon packet, when the accumulated energy arrives at a sufficient level. Given that larger vibration intensity gives higher harvested power, the packet count within a constant time interval should be positively related to the road roughness. Lab testing shows the feasibility of the proposed design. In addition, this study also provides a new design scheme and easy implementation of battery-free or energy-constrained IoT systems.**

I. Introduction

Up to now, the most commonly used energy supply for Internet of Things (IoT) devices is chemical batteries. Owing to the advancements in low-power and miniature electronics, these battery-powered devices can keep alive for up to a few years [1]. However, batteries must be replaced or recharged after that. Such a maintenance task is labor-intensive, in particular, when a network contains thousands of nodes. The disused batteries are also not friendly to the environment. Therefore, the power issue impedes the further extension of IoT networks, either spatially or temporally.

Energy harvesting (EH) technology is developed to alleviate the dependence on batteries, or even get rid of the batteries, towards the battery-free IoT solutions. The most investigated ambient energy includes solar/light [2], radio frequency (RF) [3], and temperature gradient [4]. In these solutions, the extracted energy is converted into electricity with constant dc voltage to drive the digital electronics. However, most of the previous designs are taken as an alternative to their battery-powered counterparts. They simply treat an energy harvester, as well as the energy management circuit, as a stable and constant energy source. Such conventional design thinking does not fit the actual requirement of many battery-free IoT scenarios. Therefore, new guiding principles, which take both sensing requirements and energy availability into consideration, must be explored.

This study considers an application scenario of road pavement roughness estimation. Instead of thinking in a conventional way, i.e., using an energy harvester to power a commercial inertial sensor, such as accelerometers [5], [6] or gyroscopes [7], a battery-free scheme is realized by skillfully connecting the vibration intensity, harvested power, and received wireless packets. In the previous battery-powered pavement estimation systems, the accelerometer sampling rates were set to more than 100 Hz [8], [9]; therefore, such a solution consumes a large portion of the total energy. For a battery-free system, it is very difficult to provide such an amount of energy for carrying out the constant-rate sensing scheme, let alone the computational effort of the following signal processing task. On the other hand, the dynamics of an energy harvesting process also contain some aggregated information about the source vibration. Collecting such pieces of holistic information consumes much less energy than the conventional solution. Therefore, the energy harvesting process also reflects some limited but useful information of the vibration dynamics, which is induced by different pavement roughness.

II. System Design

A. Overview

Fig. 1 shows the configuration of the prototyped battery-free pavement roughness estimation system (BF-PRES). A piezoelectric structure is used as the harvesting module to extract energy from the pavement-caused vibration. Then a self-powered synchronized electric charge extraction (SP-SECE) circuit is used to efficiently convert the ac output power into dc form. The harvested energy is then stored in a storage capacitor. The following energy management circuit uses two on/off voltage thresholds to properly manage the system operation. A Bluetooth low-energy (BLE) module is used to transmit Beacon packets by consuming the harvested energy. A mobile application collects the packets and records the time intervals between every two neighboring packets. An estimating algorithm is applied to the sparsely recorded data and finally arrives at some roughness estimation results.

B. Energy Conversion and Management Circuit

In our design, the circuit can be divided into two main parts: the ac-to-dc interface circuit and power management (PM)

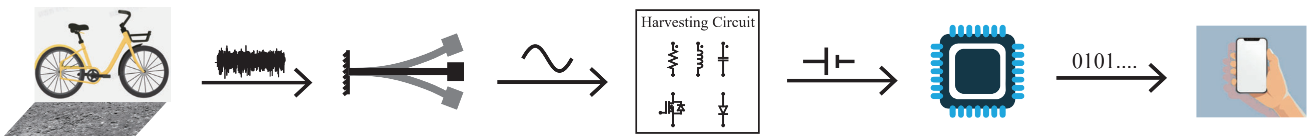

Fig. 1. BF-PRES configuration. The vibration of the bike is induced by the rough pavement. Roughness influences the harvesting power of the interface circuit, the transmission interval, therefore, is influenced.

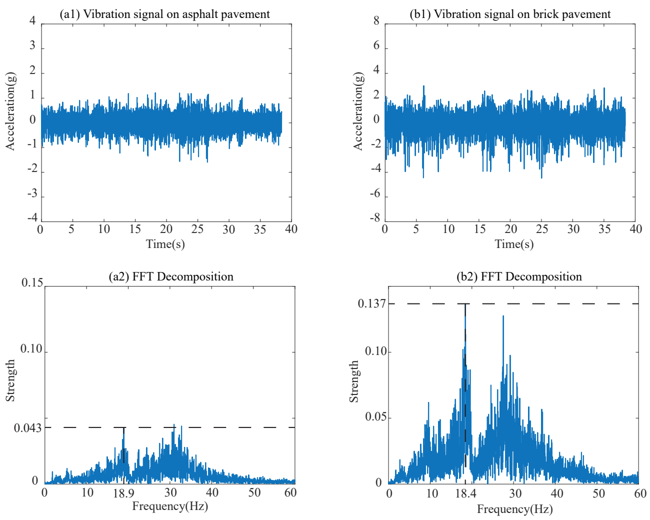

Fig. 2. Vibration data collected on asphalt and brick pavements and their corresponding FFT results. First row shows the raw acceleration data on asphalt and brick pavements, respectively; second row shows their corresponding FFT transformation results, respectively.

circuit. The interface circuit utilizes the SP-SECE technology for boosting the harvested power [10]. SECE can provide a load-independent output power without the reinforcement of additional control loops. The PM circuit contains a low-power analog UVLO (under-voltage lockout) module. The PM circuit can output a regulated 3.3 V voltage, whenever the storage (input) voltage is higher than 5 V. It can also cut off the load devices when the storage voltage is lower than 2 V. The power dissipation of the PM circuit is lower than 1 μW in typical operational conditions. Hence, the simple circuit connects the real-world vibration and the intermittent operation of the digital systems. The intermittency implies some aggregated information of the vibration.

C. Data Acquisition

A mobile app is developed to listen to the broadcasting packets from a bike-attached cell phone. Once a packet arrives, the mobile app records the arriving time. The recorded time stamps can be either used locally for visualization or sent to the cloud server for further data analysis. As the packets contain a unique field to identify the transmitter ID, multiple nodes can be implemented simultaneously. There is no need to worry about the data aliasing issue.

III. Working Principle

A. Road Vibration Pattern Analysis

The previous work on pavement roughness estimation uses the base (bike frame) acceleration to estimate the pavement conditions. With the help of the popular machine learning algorithms, the collected data was usually directly applied to either a regression or classification algorithm after pre-processing. As the raw data is time-series data, the frequency-domain pattern is easily ignored. We collect a bunch of data from different pavements and analyze it in both the time domain and frequency domain. The result is shown in Fig. 2.

It can be observed that the peak acceleration under the brick pavement is much bigger than that under the asphalt pavement. Moreover, the FFT (fast Fourier transform) result indicates that, although the pavement condition changes, the frequency distribution, as well as the peak frequencies, are approximately the same. In other words, we can use the amplitude of a dominated frequency component to distinguish different pavement conditions.

B. Self-powered Intermittent Transmission

Different from the wired- or battery-powered counterparts, the EH-powered systems usually suffer from energy starvation most of the time. The ambient source can only provide a small amount of energy in a given time interval; therefore, they mostly work intermittently. Fig. 3 demonstrates the intermittent or burst-mode working principle of an EH-powered system.

From Fig. 3, the total working process of an EH-powered system can be divided into two major phases: charge and discharge ones. A lot of research works put their focus on the latter one, i.e., to study how to extend the execution time given a fixed energy budget, or how to save and restore the execution progress among two activated phases. On the other hand, for a given harvesting circuit, the duration of the charge period more or less reflects the source condition. In vibration EH, the harvested power is closely related to the vibration intensity, i.e., the amplitudes under some specific frequencies. In other words, by studying the relation between the charge duration and the vibration condition, the vibration intensity can be estimated as a gross effect according to the wireless packets' interval.

C. Sensing Principle

To simplify the analysis, we only consider the effect of a single harmonic component from the vibrating structure. In

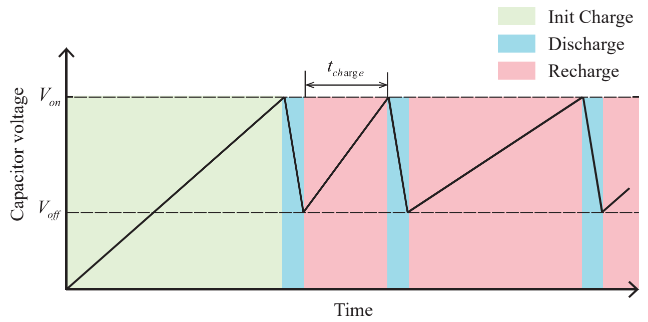

Fig. 3. The typical intermittent working process of an EH-powered system. V_{on} and V_{off} are the threshold voltages for the system to power on or power off, respectively. When the voltage across the storage capacitor reaches V_{on}, the micro-controller wakes up and starts to execute the programs. Then the buffered energy is quickly consumed; therefore, the capacitor voltage rapidly drops. When the storage voltage falls below V_{off}, the program execution stops until the next voltage recovery to V_{on}.

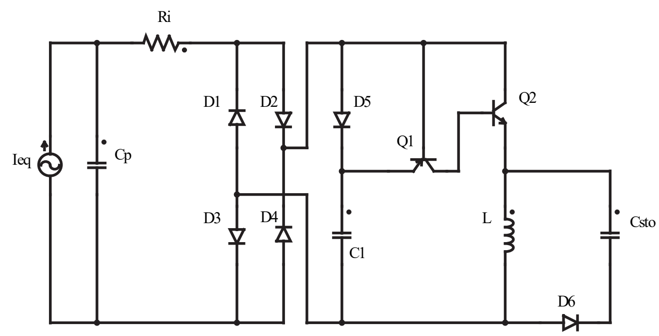

Fig. 4. Typical schematic diagram of SP-SECE circuit.

a piezoelectric structure, the open-circuit voltage magnitude across the piezoelectric beam V_{oc} is proportional to the beam deflection [11], i.e.,

$$V_{oc} = \frac{I_{eq}}{2\pi f C_p} = \frac{\alpha_e X}{C_p}, \tag{1}$$

where I_{eq} is the equivalent current source magnitude, f is the vibration frequency, C_p is the piezoelectric clamped capacitance, α_e is the voltage-to-force coupling factor, and X is the relative beam displacement (deflection), respectively. An SP-SECE circuit, which has the load-independent feature [12], is utilized to collect the harvested power. The typical schematic diagram of SP-SECE is shown in Fig. 4. SECE circuit first transfers the extracted energy from the clamped capacitance C_p to the inductor L when a voltage peak across C_p is detected. After that, the energy stored in L is transferred to the storage capacitor C_{sto} through the freewheeling diode D_6. Due to the load-independent feature of SECE, the harvested power P_h remains stable when the piezoelectric beam is subjected to the same vibration excitation. As C_p is charged in two voltage peak instants in one vibration cycle, when using SECE, P_h can be expressed as follows

$$P_h = 4 f C_p V_{oc}^2, \tag{2}$$

The energy dissipation in other modules except that in the SP-SECE circuit is ignored. We define the power conversion efficiency of the SP-SECE circuit as follows

$$\eta = \frac{P_c}{P_h} \tag{3}$$

where P_c denotes the converted power after the SP-SECE circuit. The converted power is accumulated in the storage capacitor C_{sto}.

Once the voltage across the storage capacitor C_{sto} equals to the power-on threshold V_{on}, the BLE module wakes up and starts the BLE transmission until the storage voltage V_{sto} falls below the power-off threshold V_{off}. After that, another new charge period begins. The energy consumption in one discharge phase can be calculated as follows

$$E = \frac{1}{2} C_{\text{sto}} \left(V_{\text{on}}^2 - V_{\text{off}}^2\right). \tag{4}$$

Given that P_h is an almost constant harvested power, which is independent of the loading condition, and taken constant conversion efficient η into consideration, the average charging time from V_{off} to V_{on} can be estimated as follows

$$t_h \approx \frac{E}{P_c} = \frac{E}{\eta P_h} = \frac{C_{\text{sto}}(V_{\text{on}}^2 - V_{\text{off}}^2)}{8\eta f C_p V_{oc}^2}. \tag{5}$$

Substituting (1) into (5), we have

$$t_h X^2 \approx \frac{C_p C_{\text{sto}}(V_{\text{on}}^2 - V_{\text{off}}^2)}{8\eta f \alpha_e^2}. \tag{6}$$

Since the conversion efficiency is an inherent feature of the selected SP-SECE interface circuit. All other parameters on the right-hand side are constant numbers. This inversely proportional equation relates the charging interval t_h to the square of vibration intensity X, which reflects the gross feature of pavement roughness. In general, the shorter the charging time, i.e., the smaller interval between two neighboring packets, the more severe a vibration is.

IV. Experimental Evaluation

BF-PRES is designed based on the inversely proportional relation between the wireless packets interval t_h and the square of vibration displacement magnitude X^2. We first evaluate the feasibility of this idea and use it to estimate the pavement roughness by studying the transmission intervals in a laboratory environment. Then in the field test, we apply the prototype of BF-PRES in the simulated real environment to identify three different kinds of road roughness conditions.

In the laboratory-environment experiment, we use a vibration exciter to produce vibrations at different amplitudes, in order to simulate the excitation effect under different pavement roughness conditions. Fig. 5 shows the results. The experimental results match the theoretical proportional relation, which was derived in (6), very well. Therefore, the proposed battery-free method for a coarse vibration intensity estimation is validated.

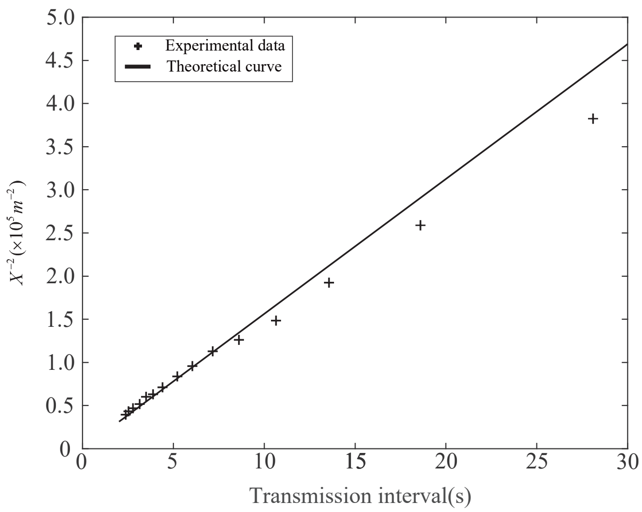

Fig. 5. Proportional relation between packets' transmission intervals and harmonic base excitation conditions.

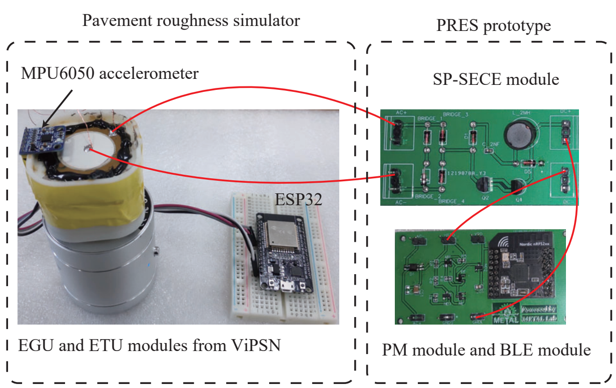

Fig. 6. Experimental setup. ESP32 and MPU6050 are used for vibration monitoring. The EGU and ETU from ViPSN platform [13] is used for pavement roughness simulation. The BF-PRES prototype consists of an SP-SECE interface circuit, a PM module, and a BLE node. It harvests energy from vibration and transmits BLE beacon packets. Any device, which can receive BLE beacon, can be used to record the time stamp for pavement roughness estimation.

After the experimental tests under the single-harmonic excitation condition in the laboratory, we further evaluate the performance of the proposed BF-PRES under an emulated multi-harmonic vibration environment. We use some modules of the ViPSN platform [13] to emulate the real vibration environment. ViPSN is an open-source platform for vibration energy harvesting system development. It contains all essential modules for developing a VEH-powered IoT system. In this study, we only use the EGU (energy generation unit) and ETU (energy transduction unit) modules to reproduce a repeatable vibration environment in the laboratory. The experimental setup is shown in Fig. 6. As analyzed in Section III, the vibration frequency distribution under different pavement roughness conditions remains quite constant. Therefore, we

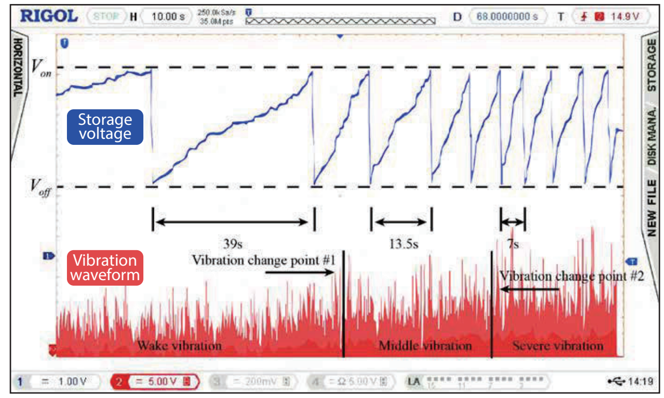

Fig. 7. The transmission interval changes when pavement roughness changes.

record a segment of the vibration signal and take it as a typical vibration pattern under the corresponding pavement condition. The vibrations at different levels are reproduced by multiplying this piece of excitation signal to three scale factors for amplification. The experimental result is shown in Fig. 7. From Fig. 7, we can observe that the vibration level changes twice at points #1 and #2, respectively. Once the pavement roughness changes, we can find an obvious change in the charging speed immediately. The transmission interval obviously changes as well. The differences of transmission intervals under different roughness conditions are also easy to detect by using many BLE devices, such as mobile phones. By listening to the packets from the BF-PRES, we have successfully realized a battery-free pavement roughness estimation system.

V. Conclusion

This paper has introduced a battery-free pavement roughness estimation system (BF-PRES). BF-PRES harvests energy from the pavement vibration and uses the harvested energy to power a BLE beacon node. Since the harvested energy is too tiny to continuously power a transmitter, the proposed design operates in an intermittent mode. It carries out one round of transmission whenever the accumulated energy is sufficient to support that specific operation. Therefore, the transmission interval is more or less related to the vibration conditions. Such a correlation gives birth to a general but useful estimation of the road roughness conditions. Powering energy-hungry sensors and the computational algorithm is unrealistic, given the limited ambient energy that can be scavenged from the physical environment. On the other hand, although we cannot obtain fine information about the vibration dynamics, coarse or general information is also valuable. The design principle of BF-PRES provides a new design thinking for energy harvesting-based wireless sensing IoT systems.

References

[1] J. Hester and J. Sorber, "The future of sensing is batteryless, intermittent, and awesome," in *Proceedings of the 15th ACM Conference on Embedded Network Sensor Systems*, 2017, pp. 1–6.

[2] M. Nardello, H. Desai, D. Brunelli, and B. Lucia, "Camaroptera: A batteryless long-range remote visual sensing system," in *Proceedings of the 7th International Workshop on Energy Harvesting & Energy-Neutral Sensing Systems*, 2019, pp. 8–14.

[3] S. Naderiparizi, A. N. Parks, Z. Kapetanovic, B. Ransford, and J. R. Smith, "Wispcam: A battery-free rfid camera," in *2015 IEEE International Conference on RFID (RFID)*, 2015, pp. 166–173.

[4] L. Sigrist, N. Stricker, D. Bernath, J. Beutel, and L. Thiele, "Thermoelectric energy harvesting from gradients in the earth surface," *IEEE Transactions on Industrial Electronics*, vol. 67, no. 11, pp. 9460–9470, 2019.

[5] P. M. Harikrishnan and V. P. Gopi, "Vehicle vibration signal processing for road surface monitoring," *IEEE Sensors Journal*, vol. 17, no. 16, pp. 5192–5197, 2017.

[6] A. S. El-Wakeel, J. Li, A. Noureldin, H. S. Hassanein, and N. Zorba, "Towards a practical crowdsensing system for road surface conditions monitoring," *IEEE Internet of Things Journal*, vol. 5, no. 6, pp. 4672–4685, 2018.

[7] A. Allouch, A. Koubâa, T. Abbes, and A. Ammar, "Roadsense: Smartphone application to estimate road conditions using accelerometer and gyroscope," *IEEE Sensors Journal*, vol. 17, no. 13, pp. 4231–4238, 2017.

[8] G. Xue, H. Zhu, Z. Hu, J. Yu, Y. Zhu, and Y. Luo, "Pothole in the dark: Perceiving pothole profiles with participatory urban vehicles," *IEEE Transactions on Mobile Computing*, vol. 16, no. 5, pp. 1408–1419, 2017.

[9] X. Zhao, X. Wu, Y.-E. Sun, H. Huang, Y. Du, and Z. Cao, "Cpdm: An efficient crowdsensing-based pothole detection and measurement system design," in *2019 IEEE 31st International Conference on Tools with Artificial Intelligence (ICTAI)*, 2019, pp. 547–554.

[10] E. Lefeuvre, A. Badel, C. Richard, and D. Guyomar, "Piezoelectric energy harvesting device optimization by synchronous electric charge extraction," *J. Intell. Mater. Syst. Struct.*, vol. 16, no. 10, pp. 865–876, 2005.

[11] J. Liang and W.-H. Liao, "Energy flow in piezoelectric energy harvesting systems," *Smart Mater. Struct.*, vol. 20, no. 1, p. 015005, Dec. 2010.

[12] C. Chen, B. Zhao, and J. Liang, "Revisit of synchronized electric charge extraction (sece) in piezoelectric energy harvesting by using impedance modeling," *Smart Materials and Structures*, vol. 28, no. 10, p. 105053, 2019.

[13] X. Li, L. Teng, H. Tang, J. Chen, H. Wang, Y. Liu, M. Fu, and J. Liang, "Vipsn: A vibration-powered iot platform," *IEEE Internet of Things Journal*, vol. 8, no. 3, pp. 1728–1739, 2020.